SURFACE FLAW DETECTION WITH FERROMAGNETIC RESONANCE PROBES

B. A. Auld, A. Ezekiel, D. Pettibone, and D. K. Winslow
Ginzton Laboratory
Stanford University
Stanford, California 94305

ABSTRACT

Ferromagnetic probes resonating at microwave frequencies have previously been shown to function as sensitive detectors of surface breaking flaws in metals. A swept frequency mode of operation was used, with the resonance line of the probe displayed on an oscilloscope and the presence of a flaw indicated by a shift of the resonance line. This type of presentation lacks good discrimination between lift-off and and flaw signals and also reduces the probe scanning speed because the entire resonance line must be swept at each measurement point on the test specimen. Our new system operates under cw conditions, with a network analyser type of display giving the probe input impedance in polar coordinates. This provides lift-off discrimination and also enhances sensitivity. Experimental curves and their theoretical interpretations will be presented, and a portable prototype instrument will be described.

INTRODUCTION

The ferromagnetic resonance (FMR) eddy current probe is a miniature microwave resonator consisting of a single crystal yttrium iron garnet (YIG) sphere, less than a millimeter in diameter (Fig. 1).

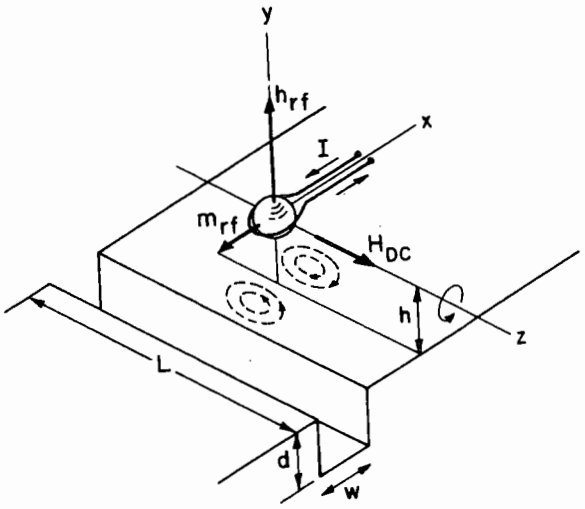

Fig. 1 General schematic of FMR probe interaction with a surface slot.

Its resonant frequency is determined not by its size, as in the case of an electromagnetic or acoustic resonator, but by the strength and direction of an applied dc magnetic field. Like an acoustic resonator, a YIG sphere has many modes of resonance and, when coupled to an external source, can be represented by the same type of equivalent circuit. With ferromagnetic resonance, the magnetization of the resonator material precesses like a spinning top about the applied dc field. For this reason, the resonant frequency is controlled by the applied field. In each mode of resonance the magnetization moves in a characteristic spatial pattern, the most important and easily excited being the one illustrated in Fig. 1, where the precession processes uniformly about the dc field.

The position of the tip of the precessing magnetization vector in Fig. 1 is described by the transverse circularly polarized magnetization m_{rf}, and it is the interaction of this rotating magnetic dipole with the test piece that generates microwave frequency (700 - 4000 MHz) eddy currents on the surface. By contrast with conventional eddy currents in the hundreds of kiloherz frequency range, these microwave eddy currents penetrated only a few microns into the surface. Nevertheless, surface breaking flaws may be detected, as in standard eddy current technology, by passing the probe over the test surface and observing the change in input impedance resulting from perturbation by the flaw of the magnetically induced surface currents. The microwave flaw signal results from the interruption of the surface currents and/or the flow of these currents into the flaw. Because of the stronger concentration of the eddy currents at the surface and also because of the resonant nature of the probe, it is expected that microwave FMR probes should have greater sensitivity to very small surface breaking cracks. A detailed analytical study of the basic probe theory presented a year ago [1] estimated that a surface breaking crack of 0.002" length should be detectable with this system. Such an estimate is, of course, incomplete in that it ignores the effects of spurious signals arising from surface roughness and lift-off variations. For this reason our top priorities this year have been to study lift-off variations and to construct a portable instrument for performing experiments under more realistic environmental conditions.

In addition to its potential advantages with regard to sensitivity the YIG probe, because of its very small size, promises to provide excellent spatial resolution, discrimination against edge effects, and accessibility to restricted corners. Figure 2 illustrates the geometries of our present generation of probes, one for surface probing and the other for the interiors of holes and corners. Our current philosophy is to apply the dc magnetic field from a separately-mounted samarium cobalt permanent magnet having dimensions in the order of a fraction of an inch. This technique, illustrated in Fig. 3, allows accessibility to flaws to be

determined by the probe size rather than the magnet.

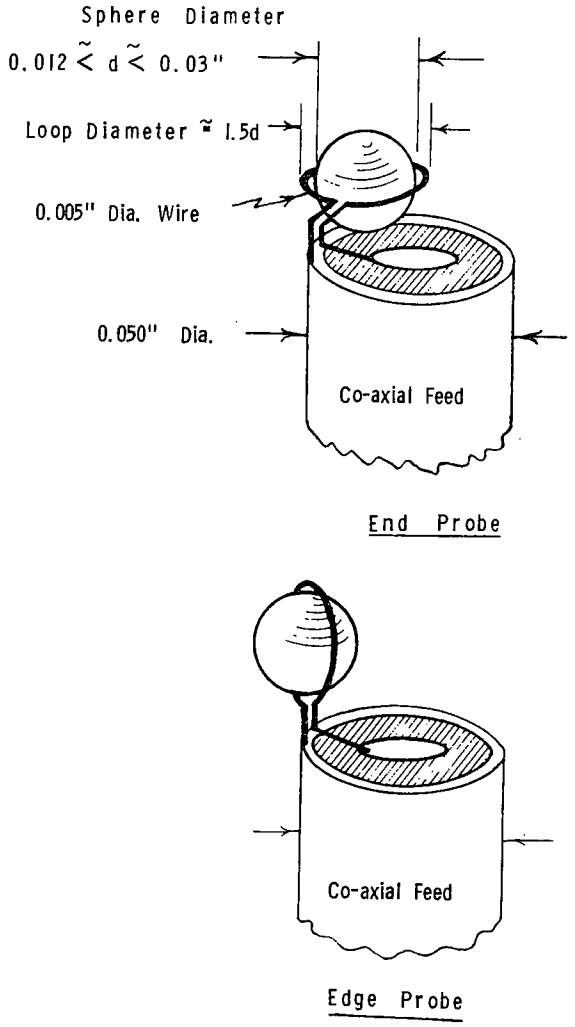

Fig. 2 Detail of currently used probes. (a) End probe. (b) Edge probe.

Unlike lower frequency eddy current probes the coil in Fig. 2 requires only a single turn, which simplifies fabrication in miniature sizes. YIG resonator technology has been an established industrial process for many years, being used for tunable microwave filter and oscillator applications. Reproducibility has therefore already been realized. At the present time the smallest YIG spheres available commercially are 0.012" diameter, but the fabrication of even smaller spheres appears feasible. This is one possible direction for further improving the edge discrimination characteristics of these probes. Another is the use of shielding, as currently applied in low-frequency probes. The lowest operating frequency in our current experiments is slightly below 800 MHz, but this is not a limit, even for the present generation of probes. Also, use of resonator shapes other than a sphere and choice of other magnetic materials offer possibilities for a very substantial lowering of the resonant frequency.

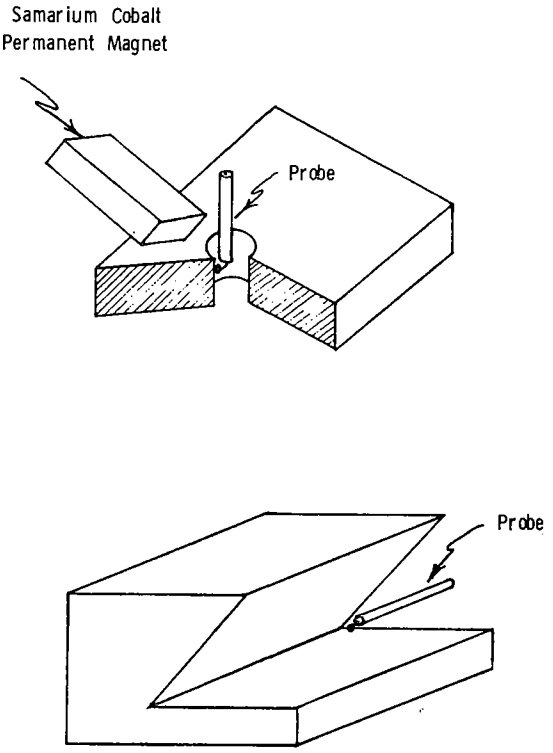

Fig. 3 Typical positioning of the edge probe relative to a test piece.

LIFT-OFF DISCRIMINATION AND FLAW SIGNAL PRESENTATION

In the last year's work the change in the input impedance due to the presence of a flaw was detected by observing the shift in the magnetic resonance frequency due to perturbation of the eddy currents. Initially the resonance line was displayed on an oscilloscope by exciting the probe at a fixed frequency and then sweeping the probe resonance by applying a swept magnetic field (Fig. 4). This was a bulky and and inconvenient technique, and later experiments were performed with a fixed magnetic field and a swept frequency source. Active probes were also constructed, in which the YIG probe controlled the frequency of a transistor oscillator. The disadvantage of these methods is that they utilize only the amplitude of the flaw signal, whereas it is well-known in low-frequency eddy current applications that the phase information provides lift-off discrimination (Fig. 5(a) and (b)), as well as flaw depth information. An improved type of probe operation, giving the required phase information, is therefore being used this year. Basically, a small dedicated network analyser provides a measure of the complex input impedance of the probe, in either fixed or swept frequency operation, and this complex impedance information is displayed on an image storage tube.

In conventional low-frequency eddy current testing the curve traced in the complex impedance plane by a variation in lift-off follows a different path than the curve traced by traversing a flaw.[2,3] Figure 5(a) and (b) compares the lift-off curves

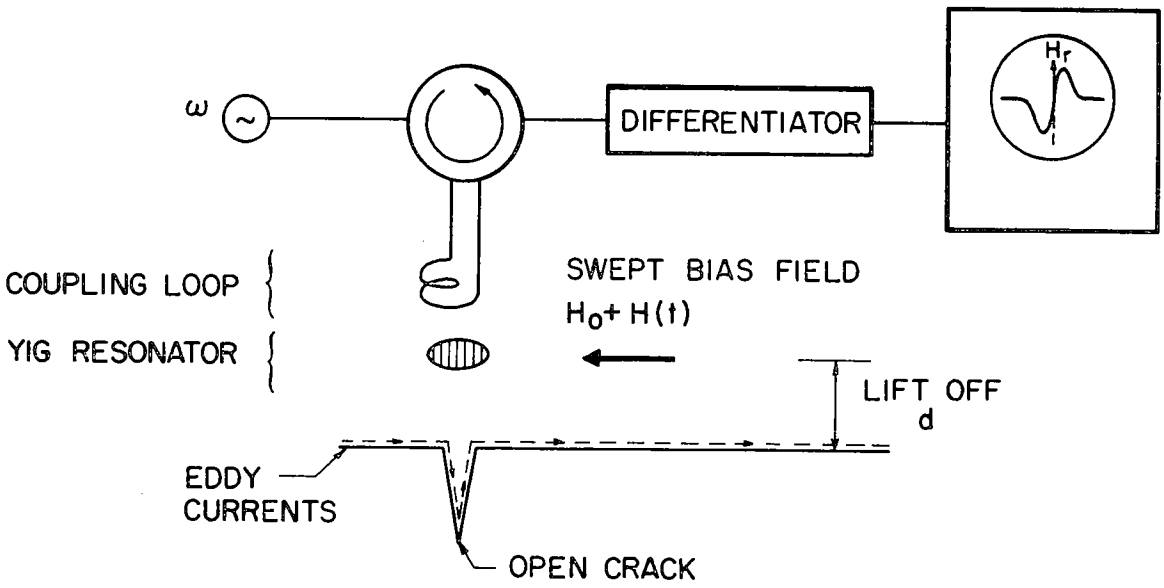

Fig. 4 Original method of flaw detection by observation of the ferromagnetic resonance frequency shift.

(dashed) with flaw signal curves (solid) for single coil and differential coil versions of a low-frequency probe. The figure-eight characteristic of the differential coil can be easily visualized by superposing two single coil responses that are 180° out of phase and occupy displaced but overlapping responses in space. In both of these figures the flaw signal has a component orthogonal to the lift-off curve, and this effect is exploited in eddy current instruments by designing the electronics so that one can select this orthogonal signal component for presentation. Corresponding impedance plane curves for the FMR probe are shown in Fig. 5 (c). As was noted in our February 1979 report,[4] the lift-off curve now follows a closed circle because of the resonance phenomenon and, with proper adjustment of the probe, the flaw curve is a teardrop more or less aligned along the lift-off curve. To obtain this type of response it appears that excitation of a second (or spurious) FMR mode, in addition to the uniform precession mode of Fig. 1, is required. Deliberate excitation of such a mode is something to be avoided in YIG filter and oscillator design, and marks a distinct difference between the operation of the YIG probe and earlier YIG devices.

The effect of spurious mode coupling on the complex impedance versus frequency curve of the YIG probe depends on the nature of the coupling. This can be best illustrated by looking at equivalent circuit models. Figure 6 shows the usual equivalent circuit representation of a low-frequency probe, where lift-off is modeled as a change in mutual inductance and conductivity changes or flaws in the test piece by changes in the load resistance. Straightforward circuit analysis shows that this circuit gives impedance curves of the type illustrated in Figs. 5(a) and (b). The FMR (or YIG) probe, on the other hand, has a main internal resonance (uniform precession) that is coupled to both the input excitation and the test piece, represented by R in Fig. 7. Coupling to a spurious mode may occur either directly from the excitation coil or indirectly through the uniform precession modes, as noted schematically in the figure by the two mutual couplings to the dashed spurious resonant circuit.

The complexity of the FMR resonator response can be appreciated by examining Fig. 8, which shows tuning curves (frequency versus magnetic field) for some of the modes of a magnetic sphere, including as a heavy line the uniform precession mode and a spurious mode of the same frequency. Spatial variations of the model fields are identified by a three-subscript system.[5] The uniform precession mode (110), shown in Fig. 9 for the tilted dc field arrangement that is found to give the best operating characteristics, has a uniform magnetization that processes around H_{DC}. The corresponding RF component of magnetization m_{RF} in the figure is uniform and circularly polarized in the plane normal to H_{DC}. The RF magnetization therefore has one polar variation, one azimuthal variation and no radial variations. Since the entire resonator structure is small compared to a wavelength, the input impedance can be obtained by a simple flux linkage calculation - leading to the coil inductance and coupled resonance terms shown in the figure. The degenerate mode illustrated in Fig. 10 is much more complicated and more difficult to couple, because of spatial cancellation of flux linkages. This mode was selected for illustrative purposes only, since it is unlikely that it is the one responsible for our experimental observations.

From the input impedance expression for the uniform precession mode in Fig. 9, it is easy to show that the corresponding equivalent circuit has an inductor in series with a parallel resonant circuit (Fig. 11). This is completely analogous to the equivalent circuit of an acoustic resonator or transducer, but with a coupling inductor instead of a coupling capacitor. Consequently, the complex impedance versus frequency curve is the offset circle diagram shown at the bottom of the figure. Regarding spurious mode coupling, one may consider separately the cases of direct coupling to the excitation loop and indirect coupling through the uniform precession mode. Simple flux linkage considerations show that these cases correspond to the equivalent circuits of Fig. 12, and a qualitative examination of the behavior of these circuits shows that the resistance, reactance and complex frequency versus frequency curves are as illustrated. As

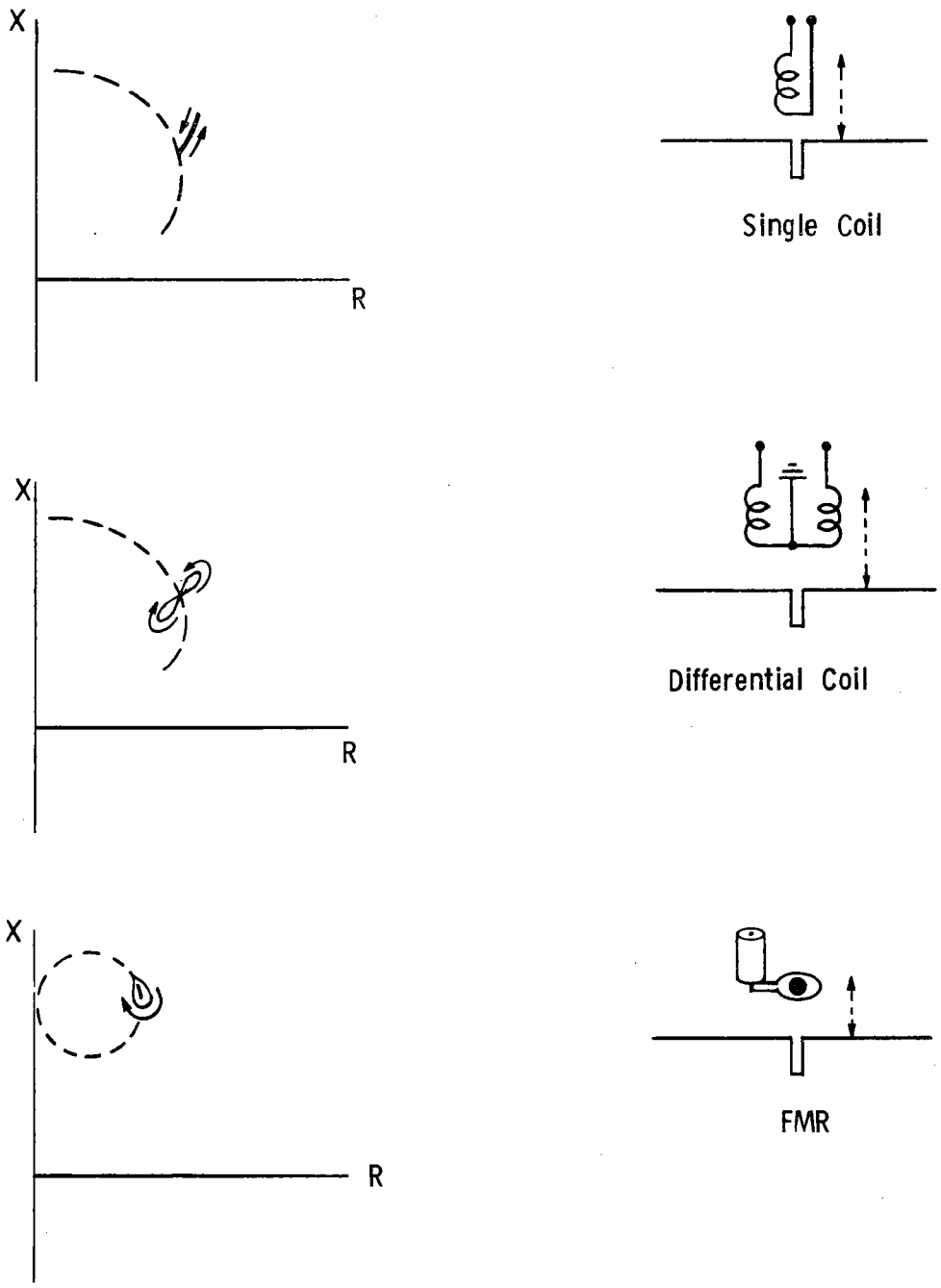

Fig. 5 Discrimination between lift-off response (dotted curve) and flaw response (solid surve) in (a) standard single coil probe, (b) standard differential coil probe, (c) FMR probe.

will be seen below, our experimental complex impedance displays correspond to the case of indirect coupling, and we therefore conclude that this is the relevant coupling mechanism. Spurious coupling in YIG filters is generally attributed to the same mechanism.

INSTRUMENTATION

As was noted above, the electronics used previously with the probe (a swept frequency source and resonance line display on an oscilloscope (Fig. 13)) does not provide the phase information necessary for lift-off discrimination. At microwave frequencies, the required complex input impedance information can be obtained by using the polar phase discriminator circuit illustrated in Fig. 14. This unit, which is the central element in commercial network analyser instruments, has as its signal input the reflected wave from the load impedance to be analysed. In the figure this is provided by the directional coupler shown at the left. The reflected microwave signal is then split and the two parts are mixed separately with a reference signal from the source, shifted 90^{o} in phase at one of the mixers. The dc outputs of the mixers are then proportional to components of the reflected signal 90^{o} out of phase with each other. Application of these

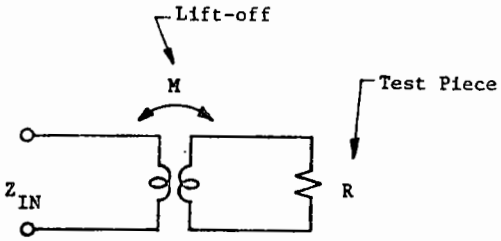

Fig. 6 Equivalent circuit model of the standard single coil probe.

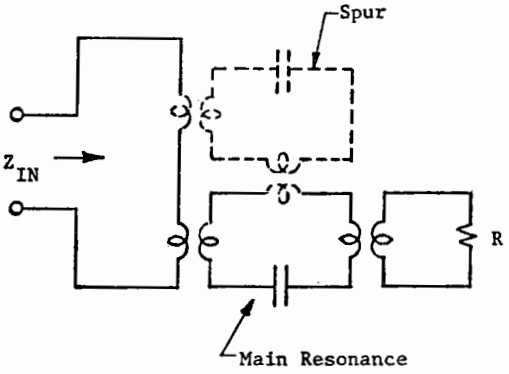

Fig. 7 Equivalent circuit model of the FMR probe.

signals to the x and y axes of an oscilloscope gives a complex display of the reflected signal and therefore of the reflection coefficient Γ_{IN}, within an arbitrary amplitude scaling and phase rotation. The relation of this display to input impedance Z_{IN} can be deduced by inverting the complex reflection coefficient relation

$$\Gamma_{IN} = \frac{Z_{IN} - Z_0}{Z_{IN} + Z_0}$$

or, better, by constructing the contours of constant R and constant X in the complex reflection coefficient plane. This leads to a system of orthogonal circular contours, known as a Smith Chart. Figure 15 compares the impedance versus frequency trajectories for the uniform precession mode coupled with a spurious mode, as displaced on a rectangular display and a Smith Chart display.

The block diagram of the dedicated network analyser constructed for use with our FMR probes is shown in Fig. 16. A small varactor-tuned transistor oscillator capable of operating from 800 to 1600 MHz serves as the source and the phase discriminator is a compact commercial unit. Use of miniature directional couplers allows the whole system to be assembled in a portable unit (Figs. 17 and 18). The electronics provides for rotation of the impedance display on the screen so that the part of the flaw signal orthogonal to the lift-off curve appears on only one axis. Gain and offset controls are also provided for magnifying the important part of the impedance curve.

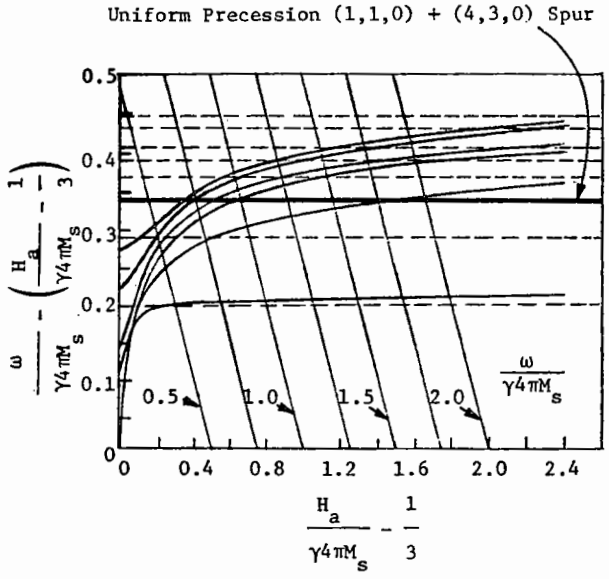

Fig. 8 Chart showing the ferromagnetic resonance frequencies of a spherical resonator as a function of the applied dc field H_a. The dashed lines represent tracking modes and the solid lines nontracking modes.

EXPERIMENTAL RESULTS

The experimental results obtained with our new instrumentation and probe configurations are not substantially different than those presented in our February report[4] and measured with a commercial network analyser. We now have a lower noise level and better display capabilities because of the offset controls available in our electronics. The same micromanipulator is used for lift-off and scan control, but the new magnet mounting allows more flexible magnetic field adjustment (Fig. 19).

Figure 20 shows a Smith Chart display of the probe input impedance, with the magnetic field adjusted for simultaneous coupling to many spurious modes. The similarity to the indirect coupling curves of Fig. 12 should be noted. Measurements with our new system of two samples discussed in our February report are shown in Figs. 21 and 22. These were both stored on the CRT before photographing. The improvement in signal-to-noise is especially notable in the second sample, although no special filtering has been used.

DIRECTIONS FOR FUTURE DEVELOPMENT OF PROBE THEORY

In Reference 1 the general theory of an FMR probe operating in the uniform precession mode was

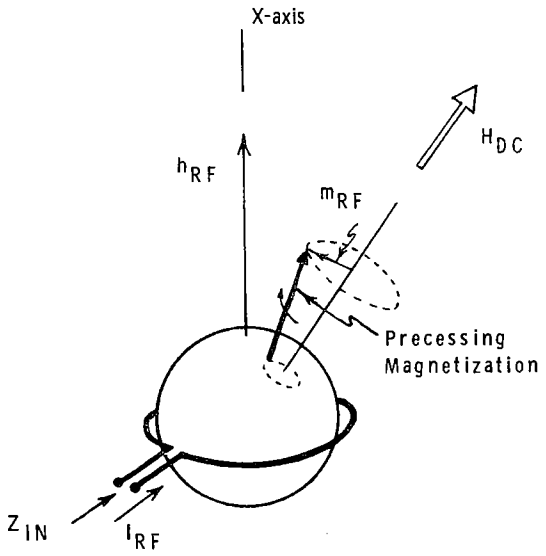

Fig. 9 Impedance at the input to the coupling coil for the uniform precession (110) mode, with the applied magnetic field at an angle.

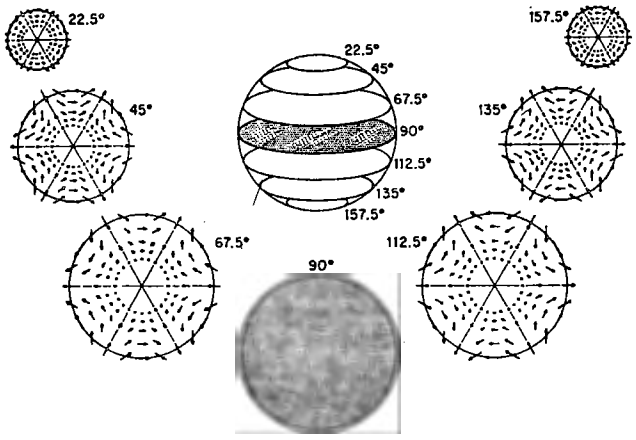

Fig. 10 Spatial distribution of the precessing magnetization in the (430) mode.

developed on the basis of a Lorentz reciprocity relation adapted to gyromagnetic materials. This theory, which was formulated for one terminal-pair probes such as the ones used here and also for two terminal pair probes having both an input and an output, is easily adapted to conventional low-frequency probes. To do so it is only necessary to reduce the gyromagnetic form of the Lorentz reciprocity relation to its ordinary form and to eliminate use of the quasistatic approximation.

This theory was applied previously only to the calculation of the frequency shifts produced by the influence of a flaw on a probe operating in the uniform precession mode. One is led naturally to ask if it can also be used to predict the results shown in Figs. 21 and 22, or to shed some light on the principles of multimode probe operation.

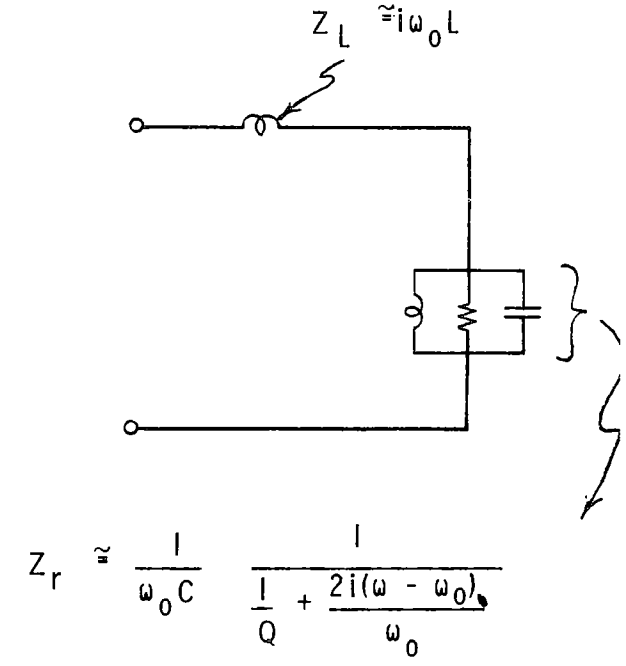

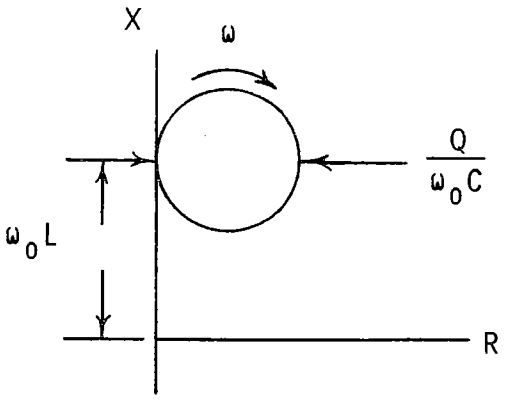

Fig. 11 Equivalent circuit and complex impedance versus frequency display for the uniform precession mode.

The previous theory was based on the construction shown in Fig. 23. Integration of the gyromagnetic Lorentz reciprocity relation over the volume enclosed by the dashed lines - taking one of the solutions in the relation to be in the presence of the flaw, the other in the absence of the flaw - gave an expression for the change in Z_{IN} at the plane S_c in terms of an integral of perturbed and unperturbed fields over the mouth of the flaw. This method does not appear to be easily adaptable to the case of a probe operating in two coupled modes.

An alternative approach would be to find for the equivalent circuit (Fig. 7) perturbations of frequency and mode coupling due to the presence of a flaw. The complex impedance curves could then be obtained from the equivalent circuit. This method

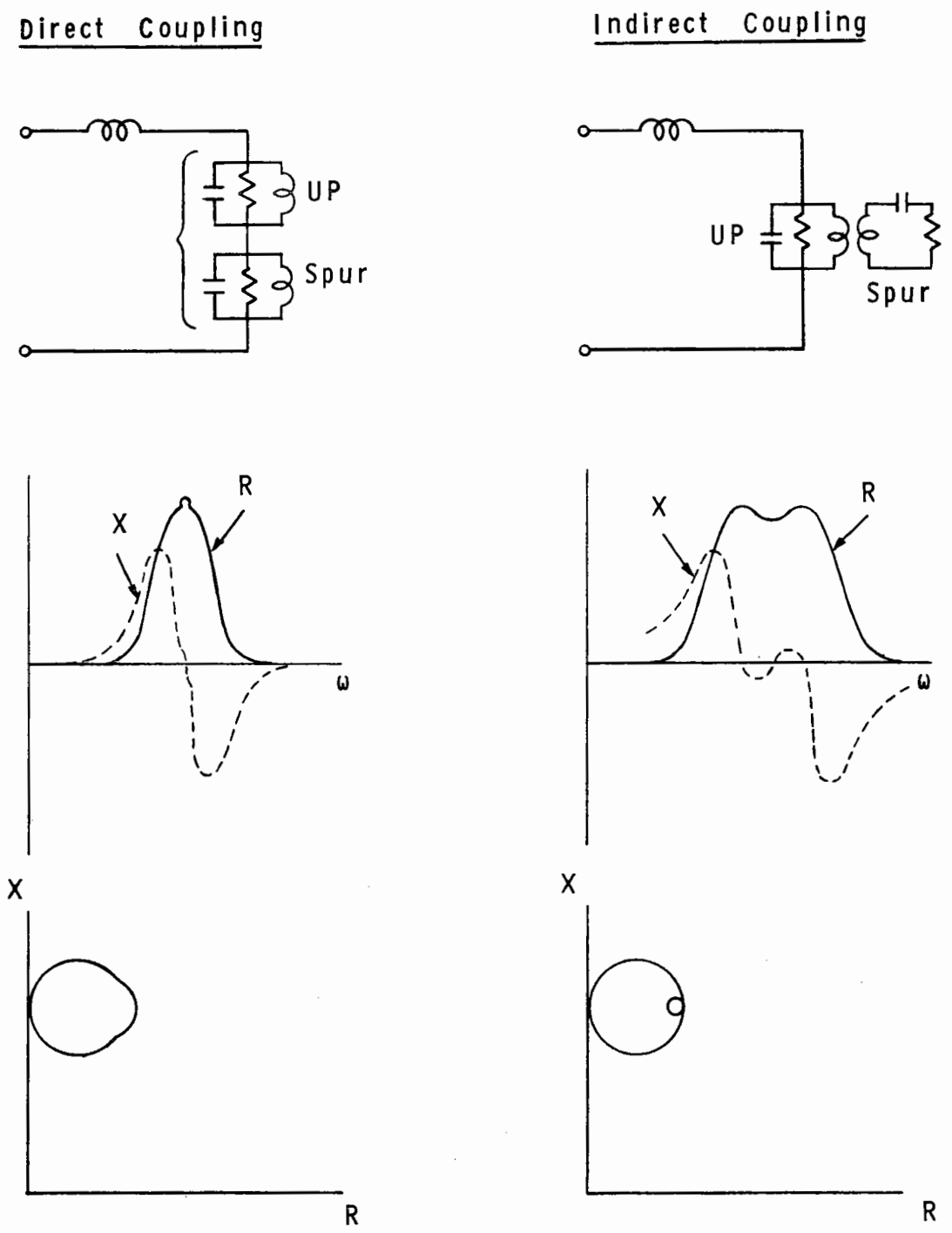

Fig. 12 Equivalent circuits and complex impedance plane displays for coupled ferromagnetic resonance modes.

might be implemented in the following way. We suppose that the plane S_c is sufficiently close to the loop that the quasimagnetostatic approximation is applicable to the entire region comprising the loop, the YIG sphere and the test piece surface. The uncoupled resonator is defined as having a short circuit at the plane S_c. Orthogonality relations for the magnetic resonance modes of this system can be derived from the quasimagnetostatic form of the complex reciprocity relation

$$\nabla \cdot (\underline{\emptyset}_1^* (i\omega_2 \underline{B}_2) + \underline{\emptyset}_2 (i\omega_1 \underline{B}_1)^*) = 0 ,$$

analogous to the corresponding relation applied to piezoelectric resonators.[6] Similarly one can develop, just as in the piezoelectric case, a modal theory for excitation of the resonator by an applied voltage at the terminal plane S_c. As in the piezoelectric case perturbation formulas may be developed for changes in the modal resonant frequencies

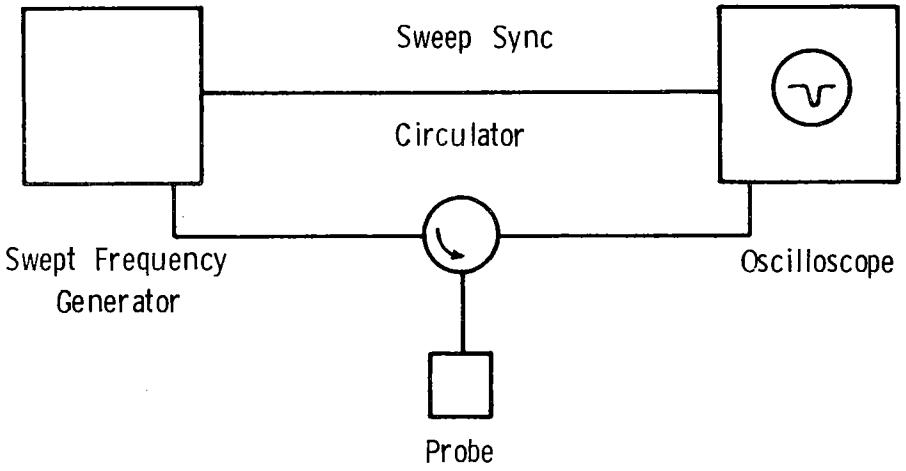

Fig. 13 Block diagram of electronics used for flaw detection by observing changes in the resonant frequency of the FMR probe.

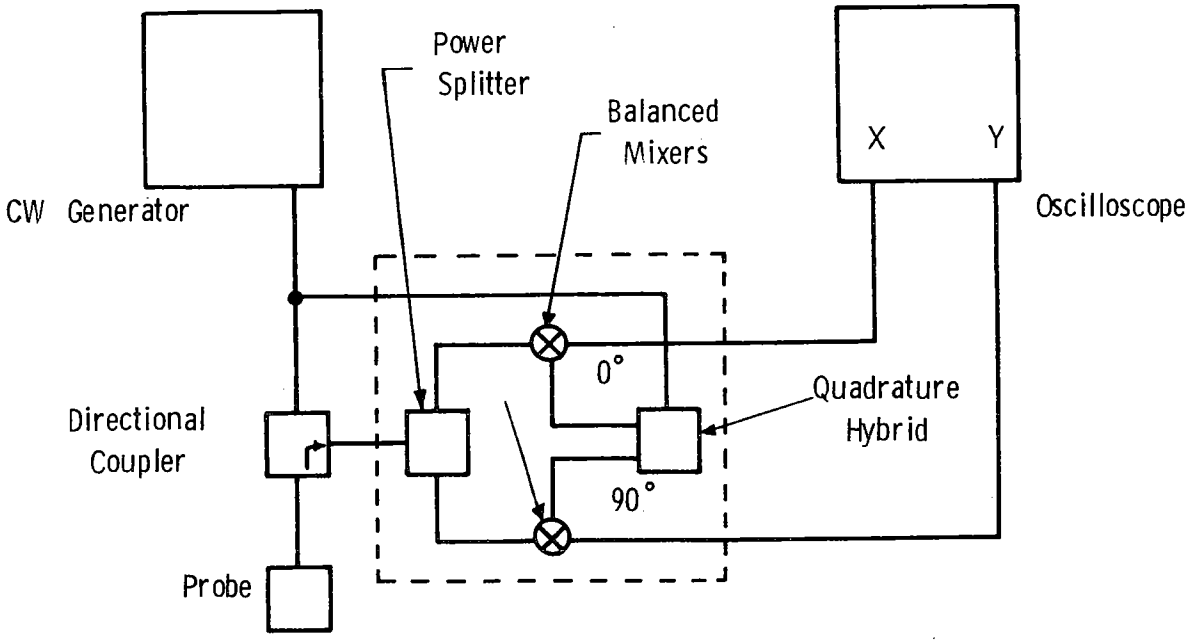

Fig. 14 Schematic of the polar phase discriminator circuit used for measuring the complex input impedance of the FMR probe.

as a function of the flaw perturbation,[7] and expressions of the same type can be formulated for mode coupling introduced by the flaw. Perturbation theory provides a useful tool for evaluating the effect of crystalline anisotropy on the probe behavior and possibly also for the effect of a nonuniform magnetic field.

SUMMARY

A portable instrument has been developed for measuring the complex input impedance of an FMR probe and displaying it on a storage image tube. This instrument has an improved signal-to-noise performance and gives clearer and larger displays than those reported previously. Coupling with spurious modes has been identified as probably taking place through the uniform precession mode, but this remains to be confirmed by further experiment. The basic elements of a theory for this type of probe operation have been established.

The highest priority tasks for future work are (1) development of more stable probe support and scanning mechanisms, especially for test pieces of complicated shapes, (2) measurements on fatigue cracks under tightly closed and partly opened conditions, (3) quantitative definition of operating conditions for optimum lift-off discrimination, (4) development of a theoretical base for multimode probe operation.

Acknowledgments are due to R. A. Craig and C. Fortunko for their advice and suggestions, to J. James for his expert assistance with the electronics, and to D. Walsh for probe fabrication.

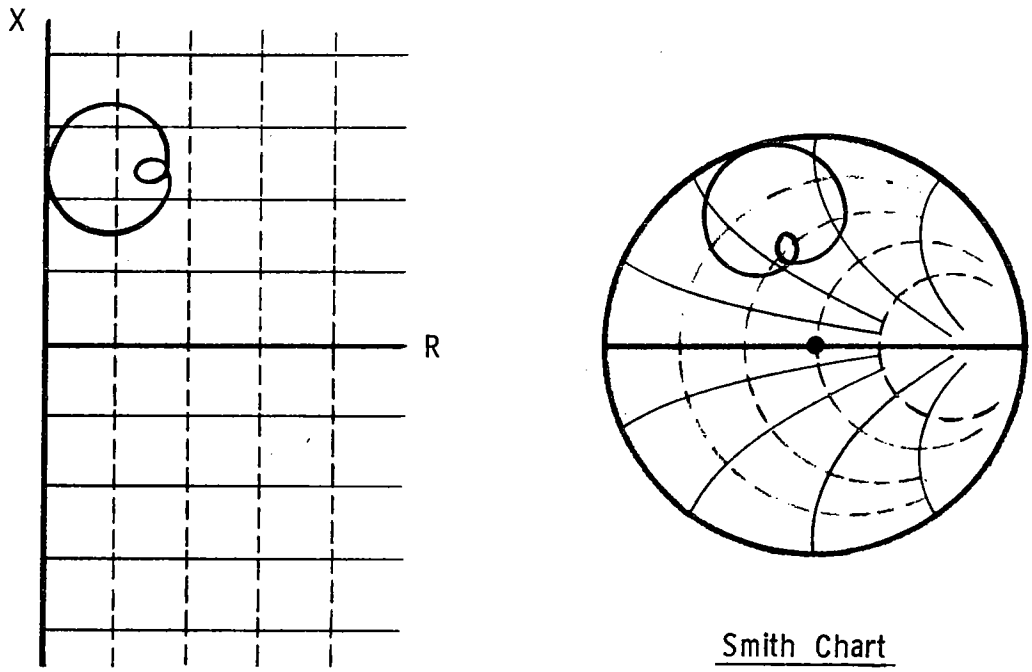

Fig. 15 Comparison of rectangular and Smith Chart complex impedance displays. Dashed lines are constant R and solid lines constant X .

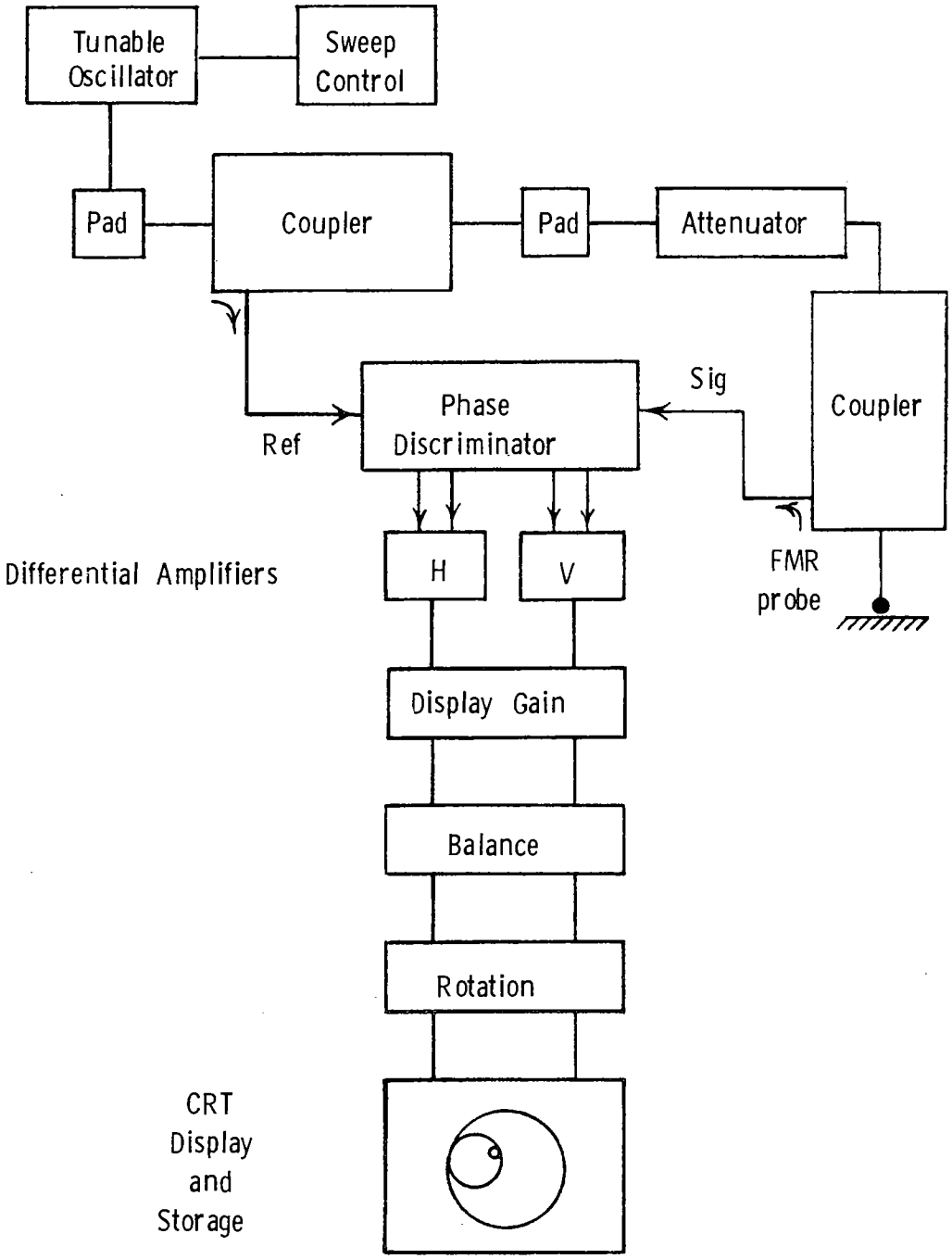

Fig. 16 Block diagram of the small dedicated microwave network analyser constructed for use with the FMR probe.

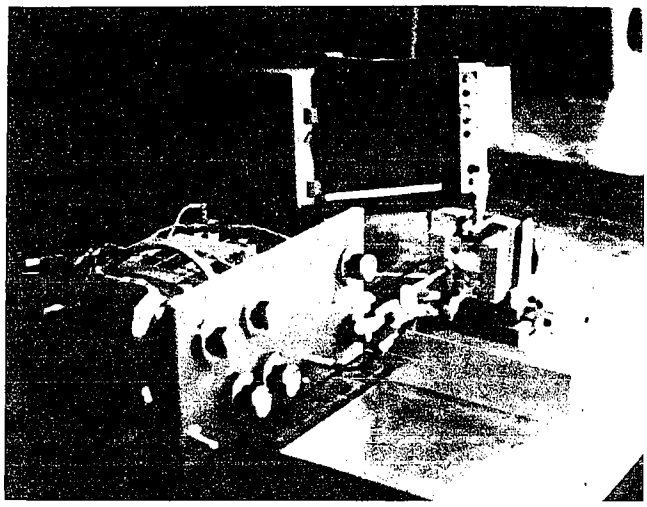

Fig. 17 Test setup, showing network analyser with case removed and storage tube for recording data.

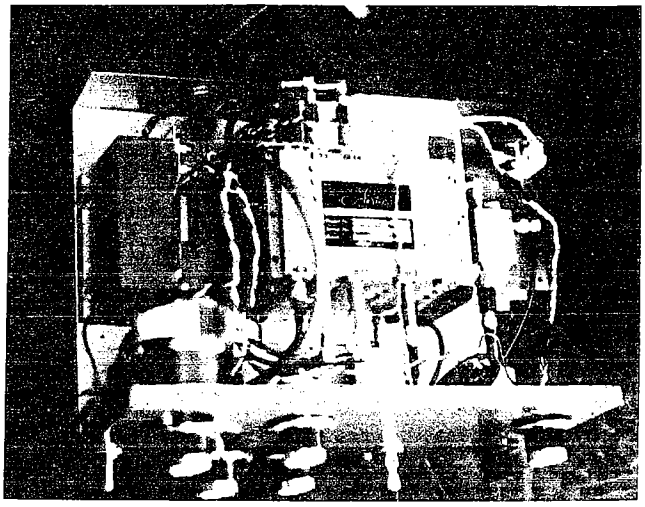

Fig. 18 Detail of network analyser circuitry.

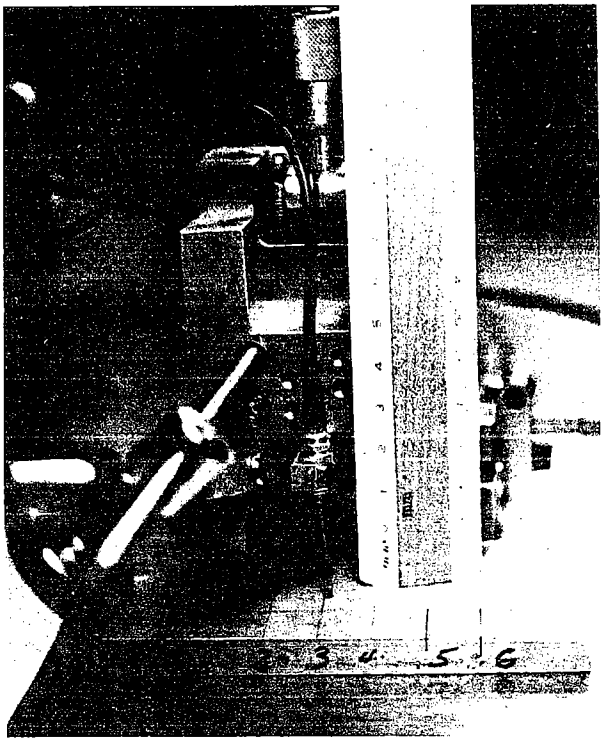

Fig. 19 Detail of probe and magnet assembly.

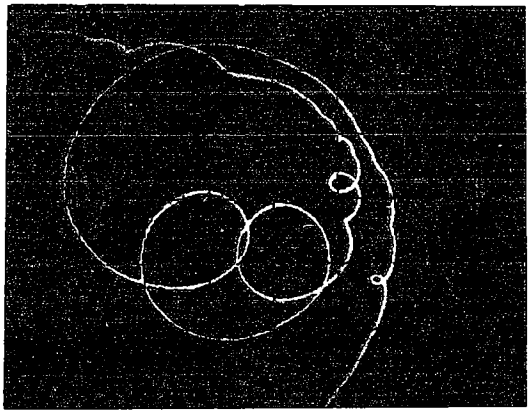

Fig. 20 Smith Chart display of probe input impedance adjusted to show many spurious mode couplings. The trace shows impedance versus frequency of the probe placed in proximity to the test piece surface.

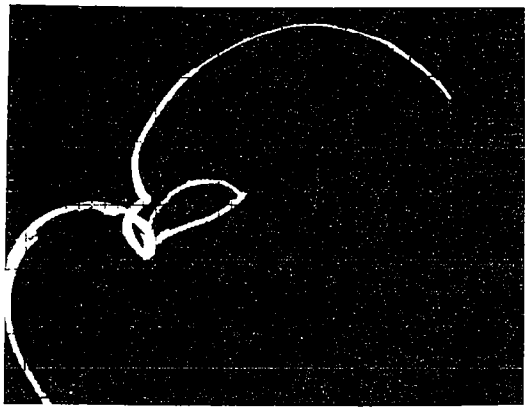

Fig. 21 Observation on test slot B-4 with length = 2", depth = 0.010" and width = 0.012", in aluminum (Fig. 19). The outer scalloped curve gives impedance versus frequency and shows an open loop corresponding to spurious mode coupling. Scanning the probe over the test slot at a fixed frequency (≈.850 MHz) produces the elliptical trace coming out of the side of the spurious mode loop.

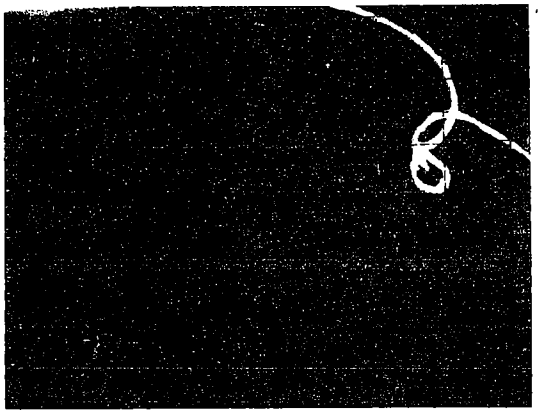

Fig. 22 Traces analogous to those of Fig. 21, but for an EDM notch (length - 0.105", depth = 0.024", width = 0.10") in titanium G-4.

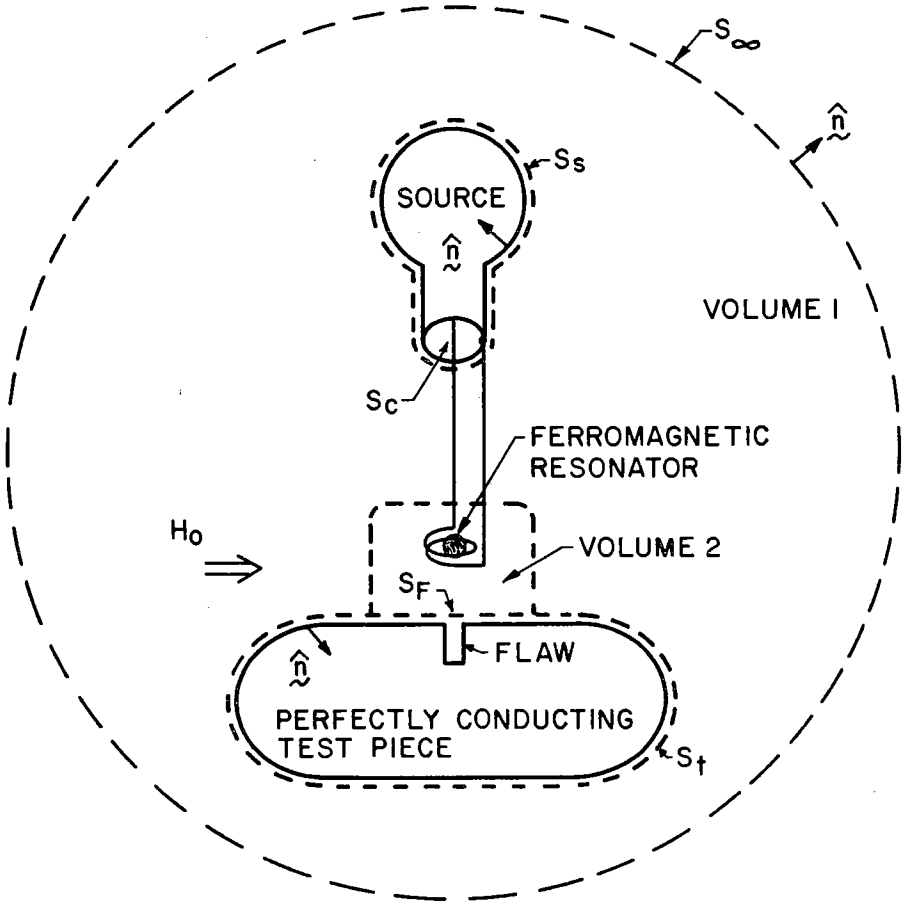

Fig. 23 Construction for the development of FMR probe theory from the reciprocity relation for gyrotropic materials.

This research was sponsored by the Center for Advanced NDE operated by the Science Center, Rockwell International, for the Advanced Research Projects Agency and the Air Force Materials Laboratory under Contract F33615-74-C-5180.

REFERENCES

1. B. A. Auld, "Theory of Ferromagnetic Resonance Probes for Surface Cracks in Metals," Ginzton Lab Report No. 2839, Contract (CMR) NSF DMR76-00726, Stanford University (July 1978).

2. H. Libby, "Introduction to Electromagnetic Nondestructive Test Methods," Wiley-Interscience, New York (1971).

3. T. J. Davis, "Multifrequency Eddy Current Inspection with Continuous Wave Methods," Proc. ARPA/AFML Review of Progress in Quantitative NDE, pp. 109-116, Science Center, Rockwell International (January 1979).

4. B. A. Auld, C. Eberspacher, A. Ezekiel, and D. Winslow, "Surface Flaw Detection with Ferromagnetic Resonance Probes," Ginzton Lab Report No. 2928, Rockwell International Science Center Grant 77-70946 (February 1979).

5. B. Lax and K. Button, "Microwave Ferrites and Magnetics," Section 4.6, McGraw-Hill, New York (1962).

6. B. A. Auld, "Acoustic Fields and Waves in Solids, Volume II," pp. 250-262, Wiley-Interscience (1973).

7. Ibid., pp. 315-324.